

# Bias-controlled intersubband wavelength switching in a GaAs/AlGaAs quantum well laser

K. Berthold, A. F. J. Levi, S. J. Pearton, and R. J. Malik  
 AT&T Bell Laboratories, Murray Hill, New Jersey 07974

W. Y. Jan and J. E. Cunningham  
 AT&T Bell Laboratories, Holmdel, New Jersey 07733

(Received 12 May 1989; accepted for publication 26 July 1989)

The light emission characteristic of a GaAs/AlGaAs single quantum well laser with an intracavity monolithic loss modulator has been investigated. Discrete, widely separated, wavelength switching from the first (875 nm) to the second (842 nm) subband is achieved by changing the applied modulator bias. In addition, we show that 2 mW of lasing light power may be modulated with a change in current of 250  $\mu$ A and a voltage change of 1 V.

Solid-state light-emitting devices with the capability of electrically controlled wavelength switching may become important for read and write operations, chip-to-chip interconnects, and wavelength division and multiplexing. With this in mind, various groups have investigated laser diode structures with double active layers and different active materials.<sup>1-4</sup> Recently, lasing from the second subband of single quantum well (SQW) diodes has been reported.<sup>5-7</sup> In these devices the use of a short cavity length<sup>5</sup> and/or narrow stripe width<sup>6,7</sup> increases losses causing lasing to occur from the second subband where there is higher gain due to the higher density of states.

In this letter we present a new technique to achieve intersubband wavelength switching in SQW laser diodes. We show that bias applied to an intracavity monolithic loss modulator induces wavelength switching from the second subband ( $n = 2$  transition) to the first subband ( $n = 1$  transition). This effect occurs because the absorption coefficient in the modulator section is sensitive to the applied modulator bias voltage. In addition, at fixed lasing wavelength, we demonstrate very efficient voltage-controlled light intensity modulation.

A schematic diagram of the device structure is shown in Fig. 1. It is a gain-guided graded index separate confinement heterostructure (GRINSCH) SQW laser grown by molecu-

lar beam epitaxy on a semi-insulating (100) oriented GaAs substrate. The GaAs quantum well is  $\sim 110$  Å thick and is sandwiched between two 2000-Å-thick graded Al<sub>x</sub>Ga<sub>1-x</sub>As waveguide regions where the Al concentration varies from  $x = 0.2$  to 0.55. Electrical contact to the top  $p^+$ -GaAs layer is achieved using three photolithographically defined metal stripes of width  $W$ . The gap between the metal stripes is 2  $\mu$ m and the length of the small segment is  $L_A$ . Using the metal stripes as an etch mask, the GaAs cap layer is removed with a selective chemical etch. Following this an oxygen ( $O^+$ ) implant is performed to electrically isolate the metal stripes (with care being taken to ensure that the  $O^+$  implant does not extend into the active region). The resulting resistance between the segments is typically  $R > 100$  M $\Omega$ . As illustrated in Fig. 1, the two large metal stripes are electrically connected and defined as the gain region, whereas the small segment is defined as the modulator absorber region. With additional processing, electrical contact is made to the  $n^+$  layer. Finally, the wafers are cleaved into devices with a cavity length  $L_C \sim 500$   $\mu$ m.

The single facet pumped current-light characteristic under various bias conditions of a device with a stripe width  $W = 20$   $\mu$ m, an absorber length  $L_A = 20$   $\mu$ m, and a cavity length  $L_C = 500$   $\mu$ m is shown in Fig. 2. Curve (I) shows the current-light characteristic for a forward-biased absorber with  $I_A = +15$  mA. A threshold current of  $I_{G,th} = 80$  mA is measured and the lasing wavelength is  $\lambda = 869$  nm, corre-

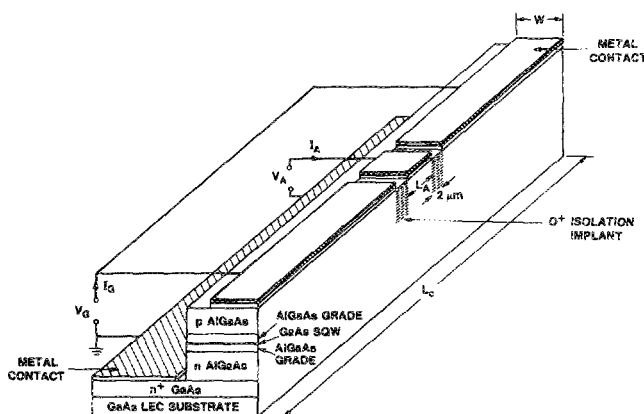


FIG. 1. Sketch of a gain-guided GaAs/AlGaAs GRINSCH SQW laser with a stripe width  $W$ , a cavity length  $L_C$ , and absorber length  $L_A$ . The gain current  $I_G$  into the large segments, the absorber voltage  $V_A$ , and absorber current  $I_A$  at the small segment are indicated.

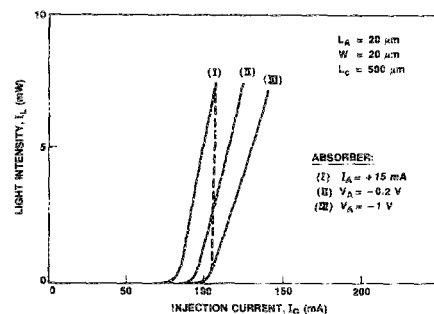


FIG. 2. Current  $I_G$  vs light intensity per facet  $I_L$  for three different absorber voltages. Curve (I) corresponds to a forward bias  $V_A$  with an injection current  $I_A = +15$  mA. Curves (II) and (III) represent the current-light characteristic for an absorber voltage  $V_A = -0.2$  V and  $V_A = -1$  V, respectively. The stripe width is  $W = 20$   $\mu$ m, the cavity length  $L_C = 500$   $\mu$ m, and the absorber length  $L_A = 20$   $\mu$ m.

sponding to lasing from the first ( $n = 1$ ) quantized state in the GaAs quantum well. However, when the absorber is reverse biased [ $V_A = -0.2$  V in curve (II) and  $V_A = -1$  V in curve (III)] the threshold current increases [ $I_{G_{th}} = 90$  mA and  $I_{G_{th}} = 100$  mA for curves (II) and (III), respectively]. The modulation of threshold current with absorber bias voltage may be explained by electroabsorption in the absorber region due to the quantum-confined Stark effect<sup>8</sup> and band-gap shrinkage in the gain region.<sup>9,10</sup> Thus, efficient modulation of the emitted light intensity at a constant gain current may be achieved in SQW lasers by reverse biasing the small absorber region. This modulation is illustrated schematically by the broken vertical line in Fig. 2.

The measured modulation of the emitted light intensity per facet as a function of absorber bias voltage  $V_A$  is presented in Fig. 3(a) for three different gain currents. At a constant current  $I_G = 105$  mA, the emitted light intensity may be reduced by more than an order of magnitude from its value at  $V_A = 0$  V by applying a reverse bias absorber voltage  $V_A = -1.2$  V. This behavior clearly demonstrates efficient voltage-controlled lasing amplitude modulation.

The total emitted light intensity versus absorber current for two different gain currents is plotted in Fig. 3(b). In both curves the operation point  $V_A = 0$  is indicated. The data presented in Fig. 3(b) demonstrate that the emitted lasing light intensity for  $I_L < 3$  mW can be modulated with a ratio of  $\sim 2$  mW/250  $\mu$ A. With increasing negative absorber bias voltage the photocurrent increases due to increased absorp-

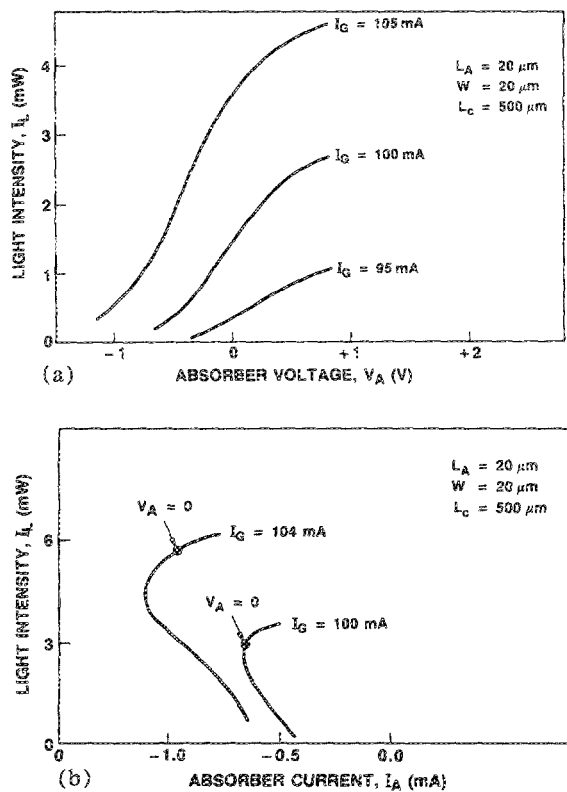


FIG. 3. (a) Emitted light intensity  $I_L$  per facet vs absorber voltage  $V_A$  for three different injection currents  $I_G$ . (b) Total emitted light intensity  $I_L$  vs absorber current  $I_A$  for two different gain currents. The operation point at  $V_A = 0$  V is indicated.

tion and enhanced collection efficiency of carriers. At high reverse bias voltages lasing is completely suppressed and the photocurrent generated is mainly due to absorption of spontaneously emitted photons in the cavity.

We also investigated the light emission characteristic of SQW lasers emitting from the second subband ( $n = 2$  transition). To observe emission from the second subband we fabricated gain-guided lasers with metal stripes of width  $W = 6 \mu\text{m}$  and cavity length  $L_C = 400 \mu\text{m}$ , thereby introducing a loss due to current spreading and lateral carrier diffusion.<sup>7</sup>

In Fig. 4 the current-light characteristic is plotted for a device with a cavity length  $L_C = 400 \mu\text{m}$  and an absorber length  $L_A = 60 \mu\text{m}$  at various absorber bias voltages. Curve (I) represents the light-current characteristic for a forward-biased absorber with  $I_A = +20$  mA. A threshold current of  $I_{G_{th}} \sim 80$  mA is measured and lasing occurs from the second subband. The nonlinearity in curve (I) is due to a spatial variation of the lasing mode.<sup>11</sup> Curves (II) and (III) show the current-light characteristic for a reverse-biased absorber with  $V_A = -0.3$  V and  $V_A = -0.7$  V, respectively. In this situation lasing occurs from the first subband.

In Figs. 5(a) and 5(b) we show the light intensity versus wavelength  $\lambda$  for two different bias conditions. In contrast to the simplest case, where one would intuitively expect a reverse-biased absorber to cause lasing from the second subband due to band filling and a forward-biased absorber to cause lasing from the first subband due to saturation of the carrier density, the experimentally observed intersubband lasing wavelength switching is explained as follows: When the gain current is increased while maintaining a constant absorber injection current  $I_A = 20$  mA, no lasing from the first subband in the fundamental transverse mode is observed due to modal losses caused by carrier-induced suppression of the refractive index and the effect of current spreading losses. At a gain current of  $\sim 80$  mA, lasing from the second subband (in the fundamental transverse mode) starts due to higher available gain in the second subband. When the modulator is reverse biased the absorption at 842 nm is much larger than the absorption at 875 nm. This fact is confirmed by photocurrent measurements performed on

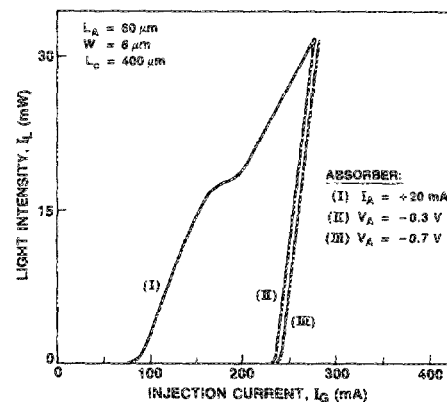


FIG. 4. Current  $I_G$  vs total emitted light intensity  $I_L$  for different absorber voltages. Curve (I) represents the light-current characteristic for a forward-biased absorber section with  $I_A = +20$  mA. Curves (II) and (III) correspond to an absorber voltage of  $V_A = -0.3$  V and  $V_A = -0.7$  V, respectively. The stripe width is  $W = 6 \mu\text{m}$ , the cavity length is  $L_C = 400 \mu\text{m}$ , and the absorber length is  $L_A = 60 \mu\text{m}$ .

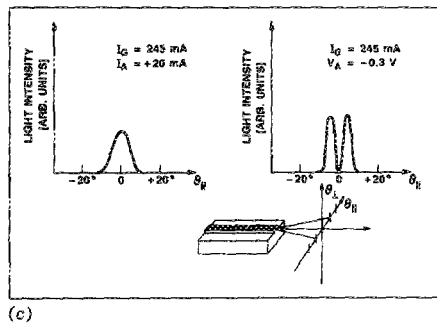
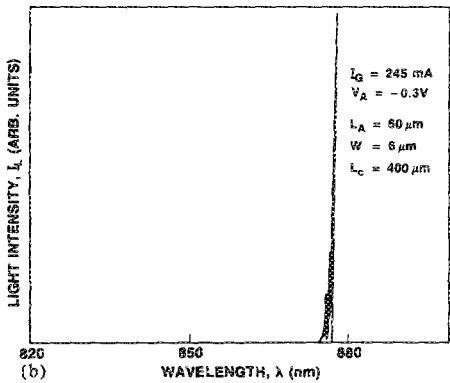
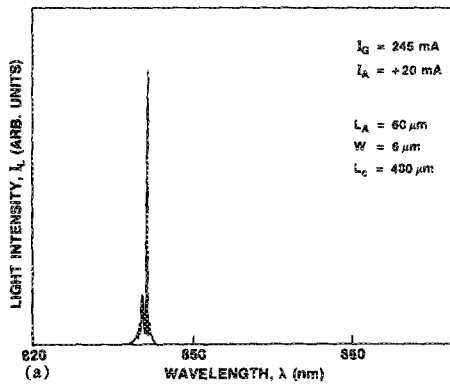


FIG. 5. (a) Light intensity  $I_L$  vs wavelength for a device with stripe width  $W = 6 \mu\text{m}$ , absorber length  $L_A = 60 \mu\text{m}$ , and cavity length  $L_C = 400 \mu\text{m}$  at a constant gain current  $I_G = 245 \text{ mA}$  and absorber current  $I_A = 20 \text{ mA}$ . (b) Light intensity  $I_L$  vs wavelength  $\lambda$  for the same device as in (a), with a gain current  $I_G = 245 \text{ mA}$  and the absorber reverse biased to  $V_A = -0.3 \text{ V}$ . (c) Measured far-field patterns parallel to the junction plane for the conditions described in (a) and (b). Also shown is a sketch of the measurement arrangement.

photodiodes fabricated from the same wafers. The measurements show that the photocurrent at 842 nm is more than one order of magnitude larger than at 875 nm under these reverse-biased conditions. Thus, lasing from the second subband is completely suppressed when the absorber is reverse biased due to the high internal loss. Lasing from the first subband in a higher-order transverse mode occurs because of the relatively low optical absorption at 875 nm and the combined and opposing influence of the gain profile and carrier-induced antiguiding inferred from the measured transverse far-field pattern [see Fig. 5(c)]. Therefore, in our structures, lasing from the first subband only occurs in higher order transverse modes which require high carrier densities (high gain current). Lasing from both the first and second subband is observed in the intermediate gain current regime,  $I_G \sim 200 \text{ mA}$  and  $I_A \sim 2 \text{ mA}$ . It is worth noting that bias-controlled wavelength switching is observed using various metal stripe geometries with  $4 \mu\text{m} < W < 8 \mu\text{m}$  and absorber length of  $40 \mu\text{m} < L_A < 100 \mu\text{m}$ .

In summary, we have demonstrated a new method for discrete, widely separated, wavelength switching from the first (875 nm) to the second (842 nm) subband in GaAs/AlGaAs SQW lasers. Switching between the subbands is achieved by changing the bias applied to a monolithically integrated modulator. In addition, the total emitted light intensity at a given lasing wavelength may be modulated with a ratio of  $\sim 2 \text{ mW}/250 \mu\text{A}$  and voltage change as low as 1 V. Further improvements in the operating characteristics of our device are expected by making use of a buried-heterostructure configuration.

We thank J. M. Gibson for providing us with transmission electron microscopy data on our devices.

- <sup>1</sup>S. Sakai, T. Aoki, and M. Umeno, *Electron. Lett.* **18**, 17 & 18 (1982).
- <sup>2</sup>H. Nagai, Y. Suzuki, and Y. Naguchi, *Electron. Lett.* **18**, 371 (1982).
- <sup>3</sup>N. Dutta, T. Ceila, J. L. Zilko, D. A. Ackerman, A. B. Piccinilli, and L. I. Greene, *Appl. Phys. Lett.* **48**, 1725 (1986).
- <sup>4</sup>W. T. Tsang, *IEEE J. Quantum Electron.* **QE-20**, 1119 (1984).
- <sup>5</sup>M. Mittelstein, Y. Arakawa, A. Larson, and A. Yariv, *Appl. Phys. Lett.* **49**, 1689 (1986).
- <sup>6</sup>Y. Tokuda, Y. Abe, T. Matsui, N. Tsukada, and T. Nakayama, *Appl. Phys. Lett.* **51**, 1664 (1987); Y. Tokuda, N. Tsukada, K. Fujiwara, K. Hamanaka, and T. Nakayama, *ibid.* **49**, 1629 (1986).
- <sup>7</sup>N. B. Patel, T. J. Mattos, F. C. Prince, and A. S. Nunes, *IEEE J. Quantum Electron.* **QE-23**, 998 (1987).
- <sup>8</sup>J. S. Weiner, D. A. B. Miller, D. S. Chemla, T. C. Damen, C. A. Burrus, T. H. Wood, A. C. Gossard, and W. Weigmann, *Appl. Phys. Lett.* **47**, 1148 (1985).
- <sup>9</sup>Y. Arakawa, A. Larson, J. Paslaski, and A. Yariv, *Appl. Phys. Lett.* **48**, 561 (1986).
- <sup>10</sup>S. Schmitt-Rink, D. S. Chemla, and D. A. B. Miller, *Adv. Phys.* **38**, 89 (1989).
- <sup>11</sup>H. C. Casey, Jr. and M. B. Panish, *Heterostructure Lasers* (Academic, New York, 1978), p. 252.